

Research Paper

Proteomic analysis of sex differences in hyperoxic lung injury in neonatal mice

Huaiping Cheng[#], Huifang Wang[#], Chantong Wu, Yuan Zhang, Tianping Bao, Zhaofang Tian[✉]

Department of Neonatology, The Affiliated Huaian No.1 People's Hospital of Nanjing Medical University; the Pediatric Diagnosis and Treatment Respiratory Key Laboratory of Huai'an, Huai'an 223300, China.

[#]These authors contributed equally to this work as first authors.[✉] Corresponding author: Zhaofang Tian, Department of Neonatology, The Affiliated Huaian No.1 People's Hospital of Nanjing Medical University, No.1 Huanghe west road, Huaiyin District, Huai'an, Jiangsu 223300, China. E-mail: tianzhaofan@163.com.© The author(s). This is an open access article distributed under the terms of the Creative Commons Attribution License (<https://creativecommons.org/licenses/by/4.0/>). See <http://ivyspring.com/terms> for full terms and conditions.

Received: 2019.11.13; Accepted: 2020.08.24; Published: 2020.09.02

Abstract

Sex-specific differences in the severity of bronchopulmonary dysplasia (BPD) are due to different susceptibility to hyperoxic lung injury, but the mechanism is unclear. In this study, neonatal male and female mouse pups (C57BL/6j) were exposed to hyperoxia and lung tissues were excised on postnatal day 7 for histological analysis and tandem mass tags proteomic analysis. We found that the lung sections from the male mice following postnatal hyperoxia exposure had increased alveolar simplification, significant aberrant pulmonary vascularization and arrest in angiogenesis compared with females. Comparison of differentially expressed proteins revealed 377 proteins unique to female and 425 unique to male as well as 750 proteins in both male and female. Bioinformatics analysis suggested that several differentially expressed proteins could contribute to the differences in sex-specific susceptibility to hyperoxic lung injury. Our results may help identify sex-specific biomarkers and therapeutic targets of BPD.

Key words: bronchopulmonary dysplasia; hyperoxia; tandem mass tags; lung tissues; gender; proteomics

Introduction

Bronchopulmonary dysplasia (BPD) affects about 40% of neonates born before 28 weeks globally [1]. BPD is mainly caused by maternal eclampsia and ventilation and is characterized by alveolar and microvascular injury and pulmonary hypertension [2]. Despite improved perinatal care, the incidence of BPD is still high [3]. Therefore, better understanding of molecular mechanisms of BPD is important for the prevention and treatment of BPD.

Sexual dimorphism has been observed in such respiratory diseases as BPD, asthma, chronic obstructive pulmonary disease, pulmonary hypertension, lung cancer and pulmonary fibrosis [4-9]. The male has higher risk of BPD in premature neonates [10]. Variations among male and female premature newborns in the progression and outcome of BPD are intimately linked to physiological, hormonal and structural differences [11]. Moreover, increased expression of cytochrome p450 may contribute to improved outcomes in female mice [12].

A recent study showed that miR-30a was implicated in sexual dimorphism in BPD [13].

Proteomics is a promising approach for clinical and diagnostic applications by mapping proteomes from cells, tissues, and organisms for the discovery of new disease biomarkers [14]. Label-free liquid chromatography-mass spectrometry (LC-MS/MS) has been applied to reveal the pathogenesis of BPD [15]. Tandem mass tags (TMTs) have been applied in gel-free proteomic approach [16]. In this study, we employed TMTs approach to compare lung proteomic profiles of neonatal mice of different sex exposed to hyperoxia.

Materials and Methods

Animals

All animal experiments were performed at The Affiliated Huaian No.1 People's Hospital of Nanjing Medical University (Huaian, China) and the protocols

were approved by Animal Use and Care Committee of The Affiliated Huaian No.1 People's Hospital of Nanjing Medical University. A total of 32 C57BL/6J neonatal mouse pups were purchased from Animal Center of Nanjing Medical University (Nanjing, China). The sex of mice was determined by physiological observation and PCR analysis on postnatal day 7 (PND7) for Sry gene.

BPD model

Thirty-two mouse pups (16 males and 16 females) within 6 h of birth were randomly assigned to two groups for the exposure to room air (21% O₂) and hyperoxia (FiO₂ ≥ 95%) for 7 days, respectively. Hyperoxia exposure was performed in Plexiglas chambers allowing continuous monitoring and constant oxygen content (95-100% oxygen). The details of the establishment of BPD model were described previously [17]. At the end, all mice were anesthetized by sodium pentobarbital, sacrificed and the lungs were excised.

Histology analysis

The chest cavity was opened and the heart was inflated with phosphate buffered saline until the lungs turned white. The left and right upper lungs were kept at -80°C immediately. The rest of the lungs were fixed at 4°C with 4% paraformaldehyde and embedded in paraffin. The tissue was cut into sections (5 µm) and stained with haematoxylin-eosin. Radial alveolar counts (RAC) were evaluated as described previously [17]. Fifteen randomly chosen fields were observed with a 10× objective of a microscope in a blinded fashion.

Protein extraction, peptide digestion and labeling

Protein extraction and peptide digestion were performed as described previously [18]. Briefly, lung tissues were lysed in RIPA lysis buffer (Keygen Biotech), and the proteins in lysates were concentrated and digested with Trypsin Gold (Promega) for 16 h at 37°C. The digested peptides were desalted with C18 cartridge and dried by vacuum. The peptides were then labeled with TMT6/10plex™ Isobaric Label Reagent (ThermoFisher) following the manufacturer's instructions. The labeled peptides were desalted using peptide desalting spin columns (ThermoFisher, 89852).

LC-MS/MS analysis

The labeled peptides were fractionated using C18 column (Waters BEH C18 4.6×250 mm, 5 µm) at 50°C. Mobile phases A was 2% acetonitrile (pH 10.0) and B was 98% acetonitrile (pH 10.0). The solvent gradient was: 3% B, 5 min; 3-8% B, 0.1 min; 8-18% B,

11.9 min; 18-32% B, 11 min; 32-45% B, 7 min; 45-80% B, 3 min; 80% B, 5 min; 80-5%, 0.1 min; 5% B, 6.9 min. The samples were dried by vacuum and dissolved in 0.1% (v/v) formic acid. Next the samples were subjected to shotgun proteomics analyses on EASY-nLCTM 1200 UHPLC system (ThermoFisher) coupled to an Orbitrap Q Exactive HF-X mass spectrometer (ThermoFisher) as described previously [18].

Bioinformatics analyses

Bioinformatics analyses were performed as described previously [19], including hierarchical clustering analysis, gene ontology (GO) analysis (based on <http://www.geneontology.org/>), KEGG (Kyoto Encyclopedia of Genes and Genomes) pathway analysis (based on <http://www.genome.jp/kegg/>), enrichment analysis (based on Fisher's Exact Test).

Enzyme-linked immunosorbent assay (ELISA)

To confirm the differentially expressed proteins identified by LC-MS/MS, we focused on FABP4 (fatty-acid-binding protein 4) and CXCL4 (Chemokine C-X-C motif ligand 4). Lungs were homogenized in PBS (pH 7.4) and centrifuged at 10,000×g to remove insoluble debris. The levels of FABP4 and CXCL4 in lung tissues were detected by ELISA kit (Thermo Fisher Scientific, Shanghai, China) according to the manufacturer's instructions.

Statistical analysis

Data were displayed as mean ± stand derivation (SD) and analyzed by two-way ANOVA. $p < 0.05$ was considered significant.

Results

Increased alveolar simplification in male mice exposed to hyperoxia exposure

No animals in hyperoxia exposed group or control group died during the experiment. Newborn mouse pups were weighed on PND7, and mice showed significant weight loss ($p < 0.01$) after exposure to 95% O₂ for 7 days compared to room air controls (Fig. 1A). However, body weights were not different for hyperoxia-male and female mice on PND7 ($p > 0.05$). Moreover, lung weight/body weight (LW/BW) ratio increased in both male and female neonatal pups with no difference (Fig. 1B). RAC was measured to assess postnatal alveolarization. On PND7, no significant difference was observed in RAC of male and female pups kept in room air, but RAC was significantly different in male mice and female mice exposed to hyperoxia (Fig. 1C). H&E staining showed typical alveolar simplification, decreased

alveolar surface area and mild interstitial thickening after hyperoxia exposure, especially in male neonatal mice (Fig. 1D-G).

Hyperoxia led to gender differences in protein expression patterns

Compared to room air group, 1,557 proteins displayed significant expression changes (≥ 1.2 fold, $p < 0.05$) in hyperoxia group. In this cohort, 638 proteins were upregulated and 919 proteins were downregulated. Compared with the room air controls, 4 of the 1,557 identified proteins, including Myosin-4, Heavy polypeptide 7, MCG140437 and Alpha-actinin-3, were upregulated in hyperoxia-exposed males but were downregulated in hyperoxia-exposed females. Notably, fructose-bisphosphate aldolase was downregulated in hyperoxia-exposed males but was upregulated in hyperoxia-exposed females compared to control group.

GO analysis of all identified proteins showed their functional classifications (Fig. 2). In particular, we found oxidation-reduction process, proteolysis and protein phosphorylation in biological process classification, protein binding, ATP binding and zinc binding in molecular function classification, and membrane, nucleus and integral component of membrane in cellular protein classification.

Differentially expressed proteins between hyperoxia and room air exposed mice in both sexes

To limit the intrinsic gender influence, we performed the analysis of differentially expressed proteins by comparing hyperoxia-exposed group of males or females with gender-matched room air-group. Fig. 3A & B showed the volcano plot in male

and female mice, respectively. Venn diagrams highlighting the upregulated 182 proteins in female mice only, 119 proteins in male mice only, and 337 proteins in both male and female mice (total 638 upregulated proteins) (Fig. 3C), as well as down-regulated 200 proteins in female mice only, 311 proteins in male mice only, and 408 proteins in both male and female mice (total 919 downregulated proteins) (Fig. 3D) exposed to hyperoxia compared to room air controls.

Eight of the 750 proteins present significant differences between the two genders, including Alpha-1-acid glycoprotein 1, MCG1051009, Pentaxin, Alpha-1-antitrypsin 1-5, Gene trap ROSA b-geo 22, Alpha-S1-casein, MCG121569 and Exocyst complex component 3-like protein 4. The level of upregulation of Alpha-1-acid glycoprotein 1, MCG1051009, Pentaxin, Alpha-1-antitrypsin 1-5 and Gene trap ROSA b-geo 22 was significantly higher in hyperoxia-exposed males than in females, whereas the relative expression abundance of Alpha-S1-casein, MCG121569 and Exocyst complex component 3-like protein 4 was significantly lower in hyperoxia-exposed females.

GO analysis showed that the differentially expressed proteins were involved in several biological processes, including response to multicellular organismal process, immune system process and single-multicellular organism process. The most significantly affected molecular functions were calcium ion binding, enzyme regulator activity, and molecular function regulator (Fig. 4A-C). Pathway analysis by KEGG suggested that the top significantly affected pathways were complement and coagulation cascades and oxidative phosphorylation (Fig. 5A-C).

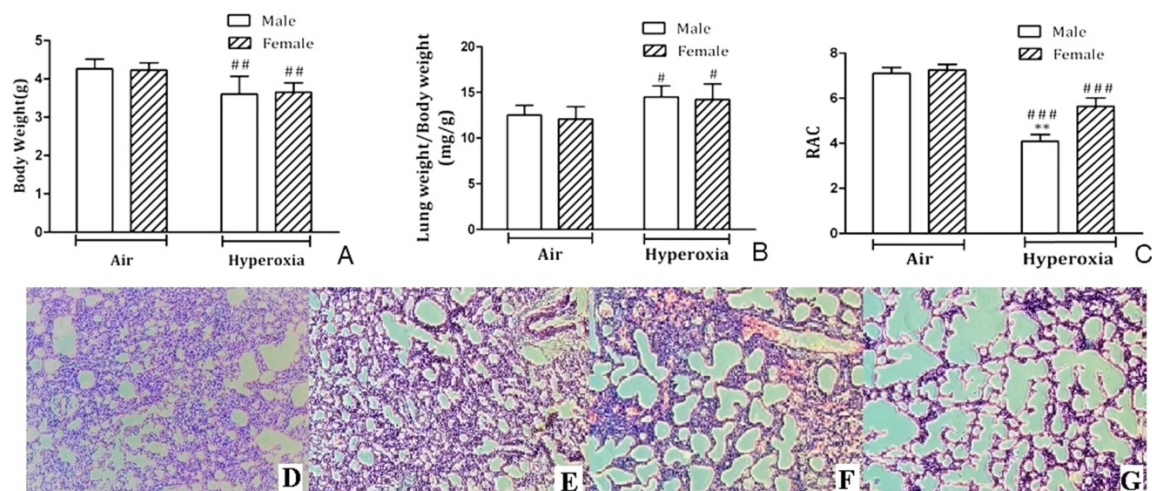


Figure 1. Histological analysis of lung tissues. **A.** Body weights of male and female postnatal day (PND) 7 mice exposed to hyperoxia or room air (n=8/group). ### $P < 0.01$. **B.** Lung weight/Body weight ratios (mg/g) in male and female neonatal mice exposed to hyperoxia on PND7 immediately after hyperoxia exposure (n=8/group). # $P < 0.05$. **C.** Radial alveolar count in male and female neonatal mice exposed to room air or hyperoxia on PND 7. ** $P < 0.01$. ### $P < 0.001$. All values are mean \pm SD (n=8). **D.** H&E staining of the lungs in female neonatal mice exposed to air. **E.** H&E staining of the lungs in male neonatal mice exposed to air. **F.** H&E staining of the lungs in female neonatal mice exposed to hyperoxia. **G.** H&E staining of the lungs in male neonatal mice exposed to hyperoxia. ($\times 100$ magnification).



Figure 2. GO annotation of all the differentially expressed proteins.

Differentially expressed proteins between hyperoxia and room air exposed male mice

Total 425 proteins were exclusively identified with significant alteration in abundance (≥ 1.2 fold, $p < 0.05$) in males in hyperoxia group. 118 proteins were upregulated while 307 proteins were downregulated. GO analysis (Fig. 4A) revealed that molecular

functions of these proteins mainly include protein binding, DNA binding, protein complex binding and actin filament binding. The mainly affected cellular component were nucleus, plasma membrane part and plasma membrane protein complex. The mainly affected biological processes were cell adhesion, chromatin remodeling and ATP-dependent chromatin remodeling, which was consistent with those of

KEGG analysis. Pathway analysis by KEGG suggested that the top 4 significantly affected canonical pathways were P53 signaling pathway, P13k-Akt signaling pathway, EGFR tyrosine kinase inhibitor resistance, and axon guidance (Fig. 5A).

Differentially expressed proteins between hyperoxia and room air exposed female mice

For females, 377 proteins were exclusively identified to be significantly altered (≥ 1.2 fold, $p < 0.05$) in the hyperoxia-exposed group. Gene ontology analysis (Fig. 4B) revealed that they also involve in several biological processes, the top three of which are response to stress, carbohydrate metabolic process and single-organism catabolic metabolic process. The top 5 most significantly affected molecular functions were oxidoreductase activity, structural constituent of ribosome, antioxidant activity, glutathione peroxidase activity and acyl-CoA oxidase activity. Pathway analysis by KEGG suggested that the top 4 significantly affected canonical pathways were

ribosome, fluid shear stress and atherosclerosis, phagosome, and amino sugar and nucleotide sugar metabolism (Fig. 5B).

Validation of changed CXCL4 and FABP4 levels in the lungs of hyperoxia exposed mice

ELISA analysis showed that CXCL4 was exclusively differentially upregulated in the lungs of hyperoxia exposed neonatal male mice compared to hyperoxia exposed female mice ($p < 0.05$) and air exposed neonatal male mice ($p < 0.05$). There was no significant difference in CXCL4 level in the lungs between hyperoxia exposed and room air exposed female mice ($p > 0.05$) (Fig. 6A). In contrast, FABP4 was exclusively differentially downregulated in the lungs of hyperoxia exposed neonatal male mice compared to hyperoxia exposed female mice ($p < 0.05$) and air exposed neonatal male mice ($p < 0.05$). There was no significant difference in FABP4 level in the lungs between hyperoxia exposed and room air exposed female mice ($p > 0.05$) (Fig. 6B).

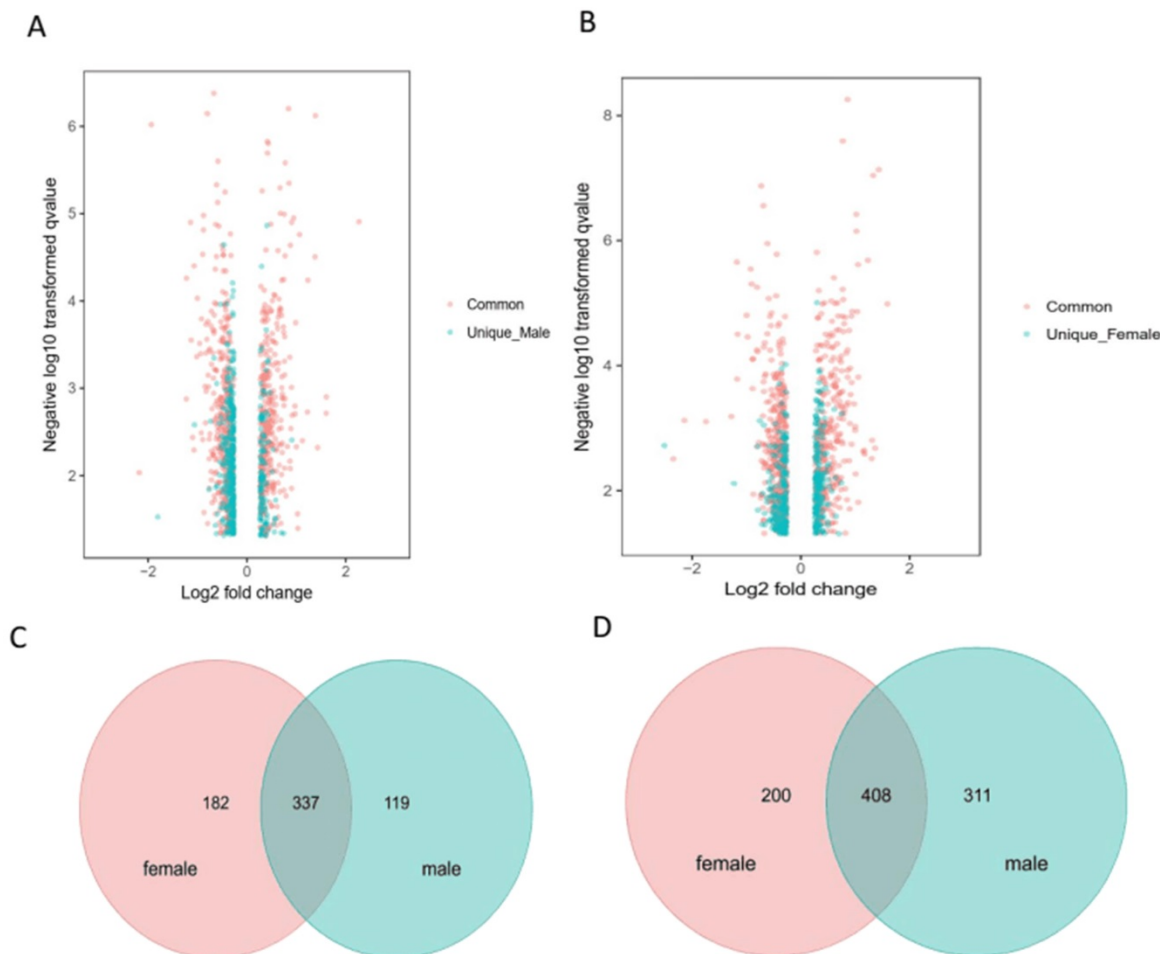


Figure 3. Distinct pulmonary proteomic patterns in male and female neonatal mice after exposure to hyperoxia. A-B. Volcano plots of the differentially expressed proteins (DEPs) in male and female neonatal mice in response to hyperoxia exposure compared to room air controls at PND7. The proteins shaded in red are common DEPs between male and female neonatal mice, whereas the proteins represented in blue are DEPs exclusive to male (A) and exclusive to female (B) neonatal mice. Venn diagrams highlighting the upregulated 182 proteins in female mice only, 119 proteins in male mice only, and 337 proteins in both male and female mice (C), downregulated 200 proteins in female mice only, 311 proteins in male mice only, and 408 proteins in both male and female mice (D) in male and female neonatal mice (PND7) exposed to hyperoxia compared to room air controls.

FABP4 is proposed as an adipokine produced in adipocytes, macrophages and endothelial cell, and is involved in the regulation of macrophages and airway inflammation [20]. FABP4 deficient mice were protected from atherosclerosis [21]. FABP4 participated in leucocyte infiltration into the airway [22]. Moreover, serum levels of FABP4 increased in many diseases including bronchopulmonary dysplasia [23]. Furthermore, serum FABP4 levels in female COPD patients increased significantly [24]. In our study, FABP4 was downregulated in male mice after hyperoxia exposure, which partially explains why neonatal male mice are more susceptible to

hyperoxia-mediated lung injury. Chemokine C-X-C motif ligand 4 (CXCL4) is a pleiotropic chemokine involved in blood coagulation, angiogenesis, tumor and immune system regulation [25,26]. In our study, CXCL4 was exclusively upregulated in hyperoxia exposed neonatal male mice. CXCL4 regulates the differentiation of monocytes by inducing a specific macrophage phenotype termed "M4". M4 macrophages are a subgroup of macrophages that express high levels of proinflammatory factors such as TNF- α and IL-6 [27]. IL-6 and TNF- α are known to be involved in sex specific hyperoxic lung injury [28].

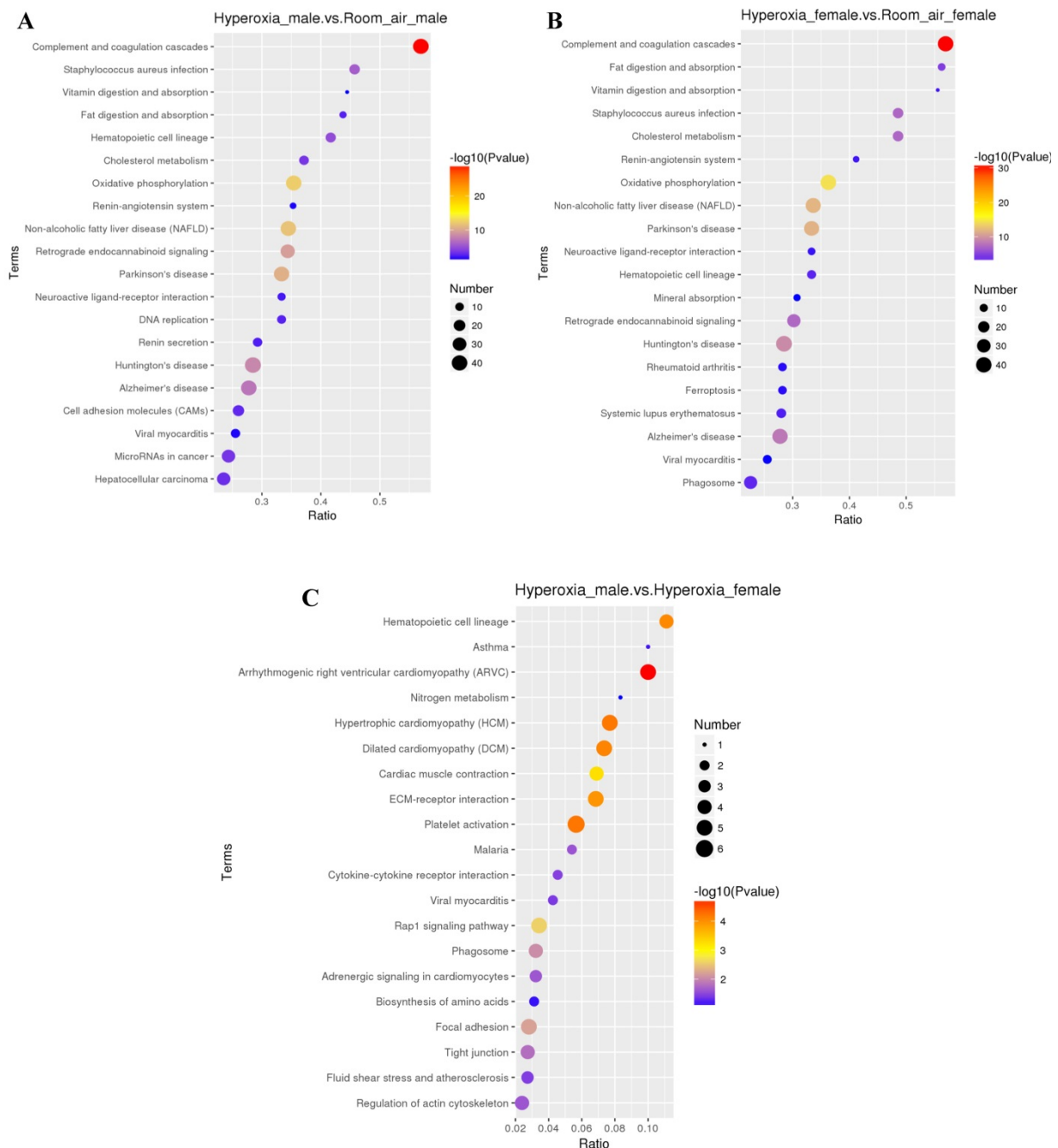


Figure 5. KEGG analysis of differentially expressed proteins. A. DEPs only in male mice. B. DEPs only in female mice. C. DEPs common in male and female mice.

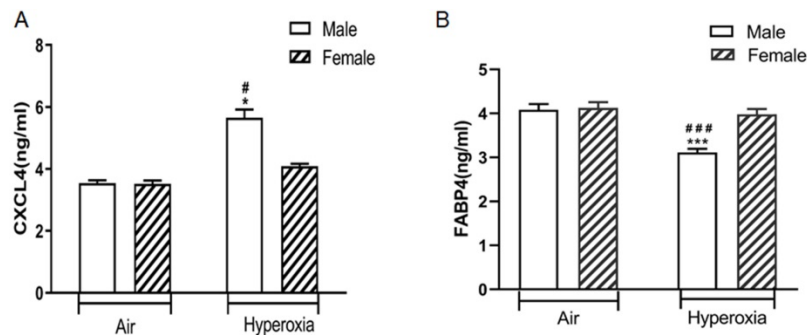


Figure 6. The levels of CXCL4 and FABP4 in lung homogenates of different groups of mice. **A.** CXCL4 level. [#]*P* <0.05 Significant differences between room air and hyperoxia exposed mice. ^{*}*P* <0.05 Significant differences between male and female mice. **B.** FABP4 level. ^{###}*P* <0.001 Significant differences between room air and hyperoxia exposed mice. ^{***}*P* <0.001 Significant differences between male and female mice. Data are presented as mean ±SD (n=8).

Pathway analysis showed sex specific differences in biological processes. Similar dysregulation in protein homeostasis and PI3K-Akt signaling pathway have been described in hyperoxic lung injury [29, 30]. Our findings are similar to the study performed in autopsy lung samples of preterm neonates on cell-cycle regulation, immune-cell regulation and sonic hedgehog signaling as differentially regulated in babies with BPD [31]. Notably, p53 pathway was upregulated in male mice while oxidative phosphorylation was downregulated in females. These data may represent ongoing apoptosis and oxidative stress in male mice, which may contribute to impaired lung development.

We also identified differentially expressed proteins common to both sexes. Calsequestrin-1 (CASQ1) is an acidic protein which binds Ca²⁺ with moderate affinity but high capacity [32,33]. We found that CASQ1 was downregulated in both male and female mice. Dainese et al. showed that the incidence of mortality in CASQ1-null mice during exposure to both halothane and heat was significantly greater in males than in females [34]. The difference in the susceptibility of CASQ1-null mice could reside in their different abilities to modulate oxidative stress [33]. The overproduction of reactive oxygen species could cause damages to lung epithelial cells [35].

In summary, we report pulmonary proteomics in mice exposed to hyperoxia. Our results show sex specific modulation of protein expression and biological processes. Comprehensive analysis of proteomic profiling would provide new insights into sex specific differences in the pathogenesis of hyperoxia induced lung injury.

Acknowledgments

Impact statement

Sex-specific differences in the severity of bronchopulmonary dysplasia were due to different susceptibility to hyperoxic lung injury, but the

mechanism is unclear. To our knowledge, this is the first report on pulmonary proteomics in mice exposed to hyperoxia. Our results show sex specific modulation of protein expression and biological processes. Comprehensive analysis of proteomic profiling provides new insights into sex specific differences in the pathogenesis of hyperoxia induced lung injury.

Author contribution

HC and HW performed most of experiments, CW, YZ, TB analyzed the data, ZT designed the study.

Funding

This work was supported by grants from the National Natural Science Foundation of China (81801495) and the Pediatric Diagnosis and Treatment Respiratory Key Laboratory of Huai'an (HAP201607).

Competing Interests

The authors have declared that no competing interest exists.

References

1. Michael Z, Spyropoulos F, Ghanta S, Christou H. Bronchopulmonary Dysplasia: An Update of Current Pharmacologic Therapies and New Approaches. *Clin Med Insights Pediatr.* 2018; 12:414454230.
2. Collins J, Tibboel D, de Kleer IM, Reiss I, Rottier RJ. The Future of Bronchopulmonary Dysplasia: Emerging Pathophysiological Concepts and Potential New Avenues of Treatment. *Front Med (Lausanne).* 2017; 4:61.
3. Doyle LW, Faber B, Callanan C, Freezer N, Ford GW, Davis NM. Bronchopulmonary dysplasia in very low birth weight subjects and lung function in late adolescence. *Pediatrics.* 2006; 118:108-113.
4. Stoll BJ, Hansen NI, Bell EF, Walsh MC, Carlo WA, Shankaran S, Laptook AR, Sanchez PJ, Van Meurs KP, Wyckoff M, Das A, Hale EC, Ball MB, Newman NS, Schibler K, Poindexter BB, Kennedy KA, Cotten CM, Watterberg KL, D'Angio CT, DeMauro SB, Truog WE, Devaskar U, Higgins RD. Trends in Care Practices, Morbidity, and Mortality of Extremely Preterm Neonates, 1993-2012. *JAMA.* 2015; 314:1039-1051.
5. Shah R, Newcomb DC. Sex Bias in Asthma Prevalence and Pathogenesis. *Front Immunol.* 2018; 9:2997.
6. Hsiao HP, Lin MC, Wu CC, Wang CC, Wang TN. Sex-Specific Asthma Phenotypes, Inflammatory Patterns, and Asthma Control in a Cluster Analysis. *J Allergy Clin Immunol Pract.* 2019; 7:556-567.
7. Docherty CK, Harvey KY, Mair KM, Griffin S, Denver N, MacLean MR. The Role of Sex in the Pathophysiology of Pulmonary Hypertension. *Adv Exp Med Biol.* 2018; 1065:511-528.
8. Tam A, Bates JH, Churg A, Wright JL, Man SF, Sin DD. Sex-Related Differences in Pulmonary Function following 6 Months of Cigarette Exposure: Implications for Sexual Dimorphism in Mild COPD. *Plos One.* 2016; 11:e164835.

9. Lim JH, Ryu JS, Kim JH, Kim HJ, Lee D. Gender as an independent prognostic factor in small-cell lung cancer: Inha Lung Cancer Cohort study using propensity score matching. *Plos One*. 2018; 13:e208492.
10. Zysman-Colman Z, Tremblay GM, Bandaeli S, Landry JS. Bronchopulmonary dysplasia - trends over three decades. *Paediatr Child Health*. 2013; 18:86-90.
11. Nemer AO, Al Anazi MS, Bhat RS, Warsy AS, Babay ZA, Addar MH, Shaik J, Al-Daihan S. Association between preterm birth risk and polymorphism and expression of the DNA repair genes OGG1 and APE1 in Saudi women. *Biocell*. 2018; 42:1-6.
12. Lingappan K, Jiang W, Wang L, Couroucli XI, Barrios R, Moorthy B. Sex-specific differences in hyperoxic lung injury in mice: implications for acute and chronic lung disease in humans. *Toxicol Appl Pharmacol*. 2013; 272:281-290.
13. Zhang Y, Coarfa C, Dong X, Jiang W, Hayward-Piatkovskiy B, Gleghorn JP, Lingappan K. MicroRNA-30a as a candidate underlying sex-specific differences in neonatal hyperoxic lung injury: implications for BPD. *Am J Physiol Lung Cell Mol Physiol*. 2019; 316:L144-L156.
14. Xiao H, Zhang Y, Kim Y, Kim S, Kim JJ, Kim KM, Yoshizawa J, Fan LY, Cao CX, Wong DT. Differential Proteomic Analysis of Human Saliva using Tandem Mass Tags Quantification for Gastric Cancer Detection. *Sci Rep*. 2016; 6:22165.
15. Yin J, Wang X, Zhang L, Wang X, Liu H, Hu Y, Yan X, Tang Y, Wang J, Li Z, Yu Z, Cao Y, Han S. Peptidome analysis of lung tissues from a hyperoxia-induced bronchopulmonary dysplasia mouse model: Insights into the pathophysiological process of bronchopulmonary dysplasia. *J Cell Physiol*. 2018; 233:7101-7112.
16. Tsuchida S, Satoh M, Kawashima Y, Sogawa K, Kado S, Sawai S, Nishimura M, Ogita M, Takeuchi Y, Kobayashi H, Aoki A, Kodera Y, Matsushita K, Izumi Y, Nomura F. Application of quantitative proteomic analysis using tandem mass tags for discovery and identification of novel biomarkers in periodontal disease. *Proteomics*. 2013; 13:2339-2350.
17. Bao TP, Wu R, Cheng HP, Cui XW, Tian ZF. Differential expression of long non-coding RNAs in hyperoxia-induced bronchopulmonary dysplasia. *Cell Biochem Funct*. 2016; 34:299-309.
18. Wei Y, Fang CL, Liu SJ, Yang WQ, Wei LS, Lei XJ, Hu F, Huang HY, Li W, Chen W, Li LM, Long YS. Long-term moderate exercise enhances specific proteins that constitute neurotrophin signaling pathway: A TMT-based quantitative proteomic analysis of rat plasma. *J Proteomics*. 2018; 185:39-50.
19. He L, He R, Liang R, Li Y, Li X, Li C, Zhang S. Protein expression profiling in the hippocampus after focal cerebral ischemia injury in rats. *J Integr Neurosci*. 2018; 17:149-158.
20. Xu H, Hertz AV, Steen KA, Wang Q, Suttles J, Bernlohr DA. Uncoupling lipid metabolism from inflammation through fatty acid binding protein-dependent expression of UCP2. *Mol Cell Biol*. 2015; 35:1055-1065.
21. Makowski L, Boord JB, Maeda K, Babaev VR, Uysal KT, Morgan MA, Parker RA, Suttles J, Fazio S, Hotamisligil GS, Linton MF. Lack of macrophage fatty-acid-binding protein aP2 protects mice deficient in apolipoprotein E against atherosclerosis. *Nat Med*. 2001; 7:699-705.
22. Shum BO, Mackay CR, Gorgun CZ, Frost MJ, Kumar RK, Hotamisligil GS, Rolph MS. The adipocyte fatty acid-binding protein aP2 is required in allergic airway inflammation. *J Clin Invest*. 2006; 116:2183-2192.
23. Parra S, Cabre A, Marimon F, Ferre R, Ribalta J, Gonzalez M, Heras M, Castro A, Masana L. Circulating FABP4 is a marker of metabolic and cardiovascular risk in SLE patients. *Lupus*. 2014; 23:245-254.
24. Zhang X, Li D, Wang H, Pang C, Wu Y, Wen F. Gender difference in plasma fatty-acid-binding protein 4 levels in patients with chronic obstructive pulmonary disease. *Biosci Rep*. 2016; 36:e302.
25. Kasper B, Petersen F. Molecular pathways of platelet factor 4/CXCL4 signaling. *Eur J Cell Biol*. 2011; 90:521-526.
26. Ruytinx P, Proost P, Van Damme J, Struyf S. Chemokine-Induced Macrophage Polarization in Inflammatory Conditions. *Front Immunol*. 2018; 9:1930.
27. Erbel C, Tyka M, Helmes CM, Akhavanpoor M, Rupp G, Domschke G, Linden F, Wolf A, Doesch A, Lasitschka F, Katus HA, Gleissner CA. CXCL4-induced plaque macrophages can be specifically identified by co-expression of MMP7+S100A8+ *in vitro* and *in vivo*. *Innate Immun*. 2015; 21:255-265.
28. Lingappan K, Jiang W, Wang L, Moorthy B. Sex-specific differences in neonatal hyperoxic lung injury. *Am J Physiol Lung Cell Mol Physiol*. 2016; 311:L481-L493.
29. Meiners S, Ballweg K. Proteostasis in pediatric pulmonary pathology. *Mol Cell Pediatr*. 2014; 1:11.
30. Reddy NM, Potteti HR, Vegiraju S, Chen HJ, Tamatam CM, Reddy SP. PI3K-AKT Signaling via Nrf2 Protects against Hyperoxia-Induced Acute Lung Injury, but Promotes Inflammation Post-Injury Independent of Nrf2 in Mice. *Plos One*. 2015; 10:e129676.
31. Bhattacharya S, Go D, Krenitsky DL, Huyck HL, Solleti SK, Lunger VA, Metlay L, Srisuma S, Wert SE, Mariani TJ, Pryhuber GS. Genome-wide transcriptional profiling reveals connective tissue mast cell accumulation in bronchopulmonary dysplasia. *Am J Respir Crit Care Med*. 2012; 186:349-358.
32. Munoz EM. Microglia-precursor cell interactions in health and in pathology. *Biocell*. 2018; 42: 41-45.
33. Michelucci A, Boncompagni S, Canato M, Reggiani C, Protasi F. Estrogens Protect Calsequestrin-1 Knockout Mice from Lethal Hyperthermic Episodes by Reducing Oxidative Stress in Muscle. *Oxid Med Cell Longev*. 2017; 2017:6936897.
34. Dainese M, Quarta M, Lyfenko AD, Paolini C, Canato M, Reggiani C, Dirksen RT, Protasi F. Anesthetic- and heat-induced sudden death in calsequestrin-1-knockout mice. *FASEB J*. 2009; 23:1710-1720.
35. Perrone S, Tataranno ML, Buonocore G. Oxidative stress and bronchopulmonary dysplasia. *J Clin Neonatol*. 2012; 1:109-114.